

Severe Hypertriglyceridemia, Reduced High Density Lipoprotein, and Neonatal Death in Lipoprotein Lipase Knockout Mice

Mild Hypertriglyceridemia with Impaired Very Low Density Lipoprotein Clearance in Heterozygotes

Peter H. Weinstock,* Charles L. Bisgaier,† Katriina Aalto-Setälä,* Herbert Radner,§ Rajasekhar Ramakrishnan,|| Sanja Levak-Frank,† Arnold D. Essenburg,† Rudolf Zechner,† and Jan L. Breslow*

*Laboratory of Biochemical Genetics and Metabolism, The Rockefeller University, New York 10021; †Department of Atherosclerosis and Therapeutics, Parke-Davis Pharmaceutical Research, Division of Warner-Lambert Co., Ann Arbor, Michigan 48105; §Institute of Pathology, Karl-Franzens University, 8010 Graz, Austria; ||Department of Pediatrics, Columbia University College of Physicians and Surgeons, New York 10032; and †Institute of Medical Biochemistry, Karl-Franzens University, 8010 Graz, Austria

Abstract

Lipoprotein lipase (LPL)-deficient mice have been created by gene targeting in embryonic stem cells. At birth, homozygous knockout pups have threefold higher triglycerides and sevenfold higher VLDL cholesterol levels than controls. When permitted to suckle, LPL-deficient mice become pale, then cyanotic, and finally die at ~ 18 h of age. Before death, triglyceride levels are severely elevated ($15,087 \pm 3,805$ vs. 188 ± 71 mg/dl in controls). Capillaries in tissues of homozygous knockout mice are engorged with chylomicrons. This is especially significant in the lung where marginated chylomicrons prevent red cell contact with the endothelium, a phenomenon which is presumably the cause of cyanosis and death in these mice. Homozygous knockout mice also have diminished adipose tissue stores as well as decreased intracellular fat droplets. By crossbreeding with transgenic mice expressing human LPL driven by a muscle-specific promoter, mouse lines were generated that express LPL exclusively in muscle but not in any other tissue. This tissue-specific LPL expression rescued the LPL knockout mice and normalized their lipoprotein pattern. This supports the contention that hypertriglyceridemia caused the death of these mice and that LPL expression in a single tissue was sufficient for rescue. Heterozygous LPL knockout mice survive to adulthood and have mild hypertriglyceridemia, with 1.5–2-fold elevated triglyceride levels compared with controls in both the fed and fasted states on chow, Western-type, or 10% sucrose diets. In vivo turnover studies revealed that heterozygous knockout mice had impaired VLDL clearance (fractional catabolic rate) but no increase in transport rate. In summary, total LPL deficiency in the mouse prevents triglyceride removal from plasma, causing death in the neonatal period, and expression of LPL in a single tissue alleviates this problem. Furthermore, half-normal levels of LPL cause a decrease in VLDL fractional catabolic rate

and mild hypertriglyceridemia, implying that partial LPL deficiency has physiological consequences. (*J. Clin. Invest.* 1995. 96:2555–2568.) Key words: lipases • lipoproteins • mice • metabolism • lipids

Introduction

Lipoprotein lipase (LPL),¹ a 52-kD protein found in association with heparan sulfate proteoglycans on endothelial cells, hydrolyzes triglycerides in chylomicrons and VLDL (for review see references 1 and 2). The human enzyme is encoded by a 4-kb cDNA (3) which encompasses 10 exons spanning 28 kb of genomic DNA on chromosome 8. The mouse LPL gene is on chromosome 8 and has the same exon-intron organization as its human counterpart (4). The two genes show 88% sequence identity in the coding region. LPL is found in almost all tissues in the body but is most abundant in adipose tissue and in skeletal and cardiac muscle. Lipolysis mediated by LPL promotes the exchange of lipids and surface apolipoproteins between lipoprotein particles, thereby affecting the size, amount, and metabolism not only of triglyceride-rich lipoproteins but of LDL and HDL as well (5). Patients with homozygous LPL deficiency (type I hyperlipoproteinemia) have severely elevated chylomicrons and VLDL and reduced LDL and HDL levels (6). Severe hypertriglyceridemia with reduced LDL and HDL can also be caused by immunological inhibition of LPL (7). A similar lipoprotein profile has been described in the *clld* mouse (8), which is both LPL and hepatic lipase deficient due to a mutation affecting lipase processing and secretion (9). Humans with heterozygous LPL deficiency have a tendency to hypertriglyceridemia with advancing age, obesity, and diabetes, as well as during metabolic stress (10–14). LPL deficiency has been suggested as a cause of familial combined hyperlipoproteinemia (FCHL) a condition characterized by increased VLDL and LDL levels due at least in part to increased hepatic secretion of apo B-containing lipoproteins (15–17). Several groups have made LPL transgenic mice (18–20) and found that LPL overexpression causes decreased triglycerides and increased HDL.

In addition to lipoprotein processing, LPL may have other functions in the body. By virtue of its ability to make fatty acids derived from hydrolyzed lipoprotein triglycerides available to underlying tissues, LPL could regulate storage in adipose tissue

Address correspondence to Dr. Jan L. Breslow, Laboratory of Biochemical Genetics and Metabolism, The Rockefeller University, 1230 York Ave., New York, NY 10021. Phone: 212-327-7704; FAX: 212-327-7165; E-mail: breslow@rockvax.rockefeller.edu

Received for publication 3 May 1995 and accepted in revised form 16 August 1995.

J. Clin. Invest.

© The American Society for Clinical Investigation, Inc.
0021-9738/95/12/2555/14 \$2.00

Volume 96, December 1995, 2555–2568

1. Abbreviations used in this paper: ES, embryonic stem; FCHL, familial combined hyperlipoproteinemia; FCR, fractional catabolic rate; HPGC, high pressure gel filtration chromatography; LPL, lipoprotein lipase; PR, production rate; RA, retinyl acetate; RP, retinyl palmitate.

or energy utilization in skeletal muscle of fat-derived calories. Thus, the absolute or relative tissue levels of LPL could play a role in obesity (21–24). Another possible function for LPL has been suggested by tissue culture studies showing that LPL can serve as a bridge between lipoprotein particles and proteoglycan matrices on cell surfaces and can augment lipoprotein uptake through both receptor-dependent and -independent mechanisms (25, 26). LPL, by virtue of its endothelial location, may be involved in localizing lipoprotein particles to the vessel wall and in promoting atherogenesis (27–30). Finally, *in vitro* and *ex vivo* experiments have shown that LPL can increase the uptake of fat-soluble vitamins A and E by a variety of cells (31). If this is the case *in vivo*, then LPL may control tissue levels of certain fat-soluble vitamins.

To rigorously test *in vivo* the various roles postulated for LPL, a line of LPL knockout mice was created. Mice completely lacking LPL are grossly normal at birth, yet within 18 h become progressively pale, develop cyanosis, and die. Their plasma shows massive hypertriglyceridemia and histological examination reveals virtually absent adipose tissue stores, severe reductions in intracellular lipid droplets in many organs such as liver and skeletal muscle, and dilated capillaries and hepatic sinusoids engorged with large lipoprotein particles. Heterozygous LPL knockout mice have moderate hypertriglyceridemia, with decreased removal but not increased synthetic rates of triglyceride-rich lipoproteins. These findings indicate a vital role for LPL in the removal of triglyceride-rich lipoproteins from mouse plasma and provide a novel animal model in which to pursue studies of postulated LPL functions in the body.

Methods

Generation of LPL-deficient mice. *pPW19.1*, a replacement-type targeting vector, was constructed from isogenic S129/J DNA in two cloning steps and included 5.5 kb of endogenous LPL gene sequences. A 1.1-kb *EcoRI* fragment containing 5' flanking and LPL exon 1 sequences preceding the translation start site was ligated upstream of the neomycin resistance gene (*neo*) in plasmid pGKNEO (32). A 4.8-kb *BamHI* fragment containing exon 2 was then subcloned downstream of *neo*. J1 embryonic stem (ES) cells (33) were cultured and selected on *neo*-resistant mouse primary embryonic fibroblasts (34). After linearization with *XhoI*, 10 μ g of targeting vector *pPW19.1* was electroporated (cell-porator from GIBCO BRL, Gaithersburg, MD) into 16×10^6 ES cells in 0.9 ml of ES cell medium (34) at 200 V and 800 μ F. Stable integrants underwent positive selection in 200, 400, or 800 μ g/ml G418 and colonies were picked into 96-well plates 10 d after electroporation. After expansion to 24-well plates, clones were trypsinized and divided to be frozen down and expanded for genomic Southern blot analysis. The correctly targeted clone was injected into C57BL/6J host blastocysts and 10–20 embryos were transferred into the uterine horn of (C57BL/6J \times CBA/J)F1 surrogate mothers (35). All resulting chimeric animals were back-crossed to C57BL/6J mice and germ line transmission was scored by coat pigment. Heterozygous mutants were identified by genomic Southern blotting of tail tip DNA and were interbred to generate homozygous mutants.

Genomic Southern blot analysis. ES cell DNA was isolated by digesting cells in lysis buffer (1% SDS, 625 μ g/ml proteinase K, 100 mM NaCl, 10 mM Tris, pH 7.5, 1 mM EDTA) at 55°C overnight and spooling genomic DNA after precipitation in ethanol. Tail tip DNA was prepared by rocking tail tips in lysis buffer (36) at 55°C overnight and spooling genomic DNA after ethanol precipitation. To screen, ES cell and mouse DNAs were digested with *NcoI* and analyzed by genomic Southern blot according to Walsh et al. (36).

Whole carcass LPL activities. 14–16-h pups were weighed and killed by decapitation. Stomachs were removed to prevent potential

contamination by ingested maternal LPL in the breast milk. Tissues were placed in 1 ml DME + 2% BSA/100 grams of carcass and underwent high speed homogenization using the Polytron homogenizer for 30 s on ice. 2 U heparin/ml of homogenate was added and samples were immediately placed at 37°C for 1 h. Samples were then spun at 3,000 rpm for 5 min at 4°C. 1 ml of supernatant was collected and respun at 12,000 rpm for 5 min at 4°C. The LPL activity in 50 μ l of supernatant was assayed as described earlier (37).

Lipid and lipoprotein analysis. Pup plasmas were obtained by killing 0- or 18-h-old litters and collecting blood via decapitation. Adult mouse blood was obtained from mice in the mornings after they had normal access to food (fed samples) and in the evening after they had fasted 8 h during the day (fasted samples). Total plasma triglyceride and cholesterol were determined enzymatically using commercial kits (No. 236691 and No. 126012, respectively; Boehringer Mannheim Corp., Indianapolis, IN). Lipoprotein cholesterol contents (profiles) were determined by on-line post-column analysis of Superose-6 gel-filtered plasma (high pressure gel filtration chromatography, HPGC). HPGC (2–20 μ l) samples were prepared by passing diluted plasma through spin filters to prevent the introduction of any obstruction to the column. Samples from *-/-* animals proved to be too lipemic to pass through the filter unimpeded, leaving a lipid residue above the filter. We assumed that the residue was composed predominantly of the abundant triglyceride-rich lipoprotein fraction, while LDL and HDL passed unobstructed, and that unless corrected, HPGC underestimated VLDL-C. Using HPGC we therefore directly quantitated LDL and HDL in these lipemic samples (unfiltered) and VLDL-C was calculated by subtraction of LDL plus HDL cholesterol from total cholesterol. Similar analyses and calculations were performed for samples obtained from *+/+* and *+/-* animals which were identical to uncorrected values obtained directly from HPGC.

Histologic analysis. After decapitation and removal of blood and tail for lipid and DNA analysis, respectively, various tissues were excised and prepared for analysis. For oil red O staining, animals were sagittally halved. One part was embedded in Tissue Tek on a cork plate, frozen in 5-methylbutan (Merck, Darmstadt, Germany), and precooled in liquid nitrogen. 4- μ m-thick sections were then cut and stained with oil red O. The remaining half was formalin fixed and embedded in paraffin wax by conventional techniques and stained with either hematoxylin-eosin, masson-trichrome, or periodic acid Schiff. For electron microscopy, tissues were diced and fixed in 2.5% glutaraldehyde in 100 mM cacodylate, pH 7.4, and postfixed in 1% osmium tetroxide in the same buffer on ice. The specimens were treated with uranyl acetate en bloc (38), dehydrated, and embedded in Epon following standard preparative procedures for electron microscopy. Semithin 1- μ m-thick sections were cut with glass knives, then stained with Azure II/methylene blue (39) for light microscope evaluation. 60–70-nm-thick sections were cut with a diamond knife on a Ultracut E ultramicrotome (Microscopical Optical Consulting, Inc., Valley Cottage, NY). The sections were collected on Formvar carbon-coated copper grids and stained with uranyl acetate and lead citrate (40) before examination with an electron microscope (100 CX; JEOL U.S.A. Inc., Peabody, MA) operated at 80 kV.

***In vivo* production and clearance of labeled VLDL.** For clearance studies, VLDL was labeled *in vivo* in control mice. Mice were injected intravenously with [3 H]palmitate (200 μ Ci) and bled 45 min later. VLDL ($d < 1.006$ grams/ml) was isolated by ultracentrifugation. Approximately 60% of radiolabeled material was associated with triglycerides, as assessed by thin-layer chromatography followed by liquid scintillation counting. Clearance of radiolabeled VLDL (3×10^5 dpm/mouse) was determined in 10 control and 10 heterozygous mice. Recipient mice received an intravenous bolus of 3 H-VLDL and were bled at 2, 5, 10, 20, 40, 75, and 120 min for determination of serum radioactivity. VLDL triglyceride kinetics were analyzed using a single- or two-pool model based on the assumption of a main VLDL pool with the remnant pool derived entirely from the main pool (41). To determine hepatic triglyceride production, three control and three heterozygous LPL-deficient mice were anesthetized and treated with Triton WR 1339

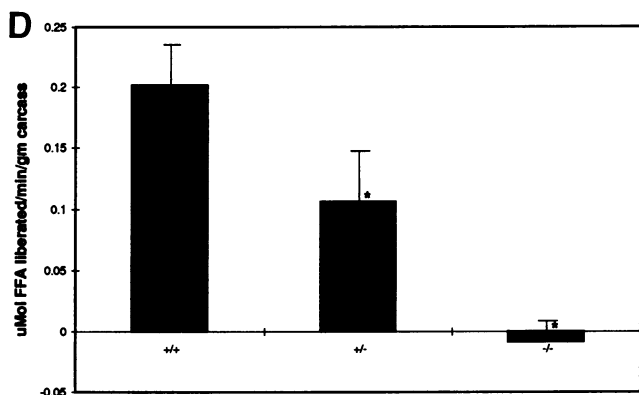
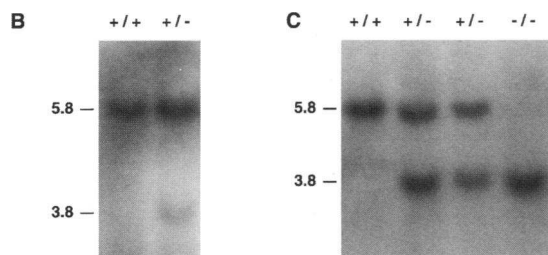
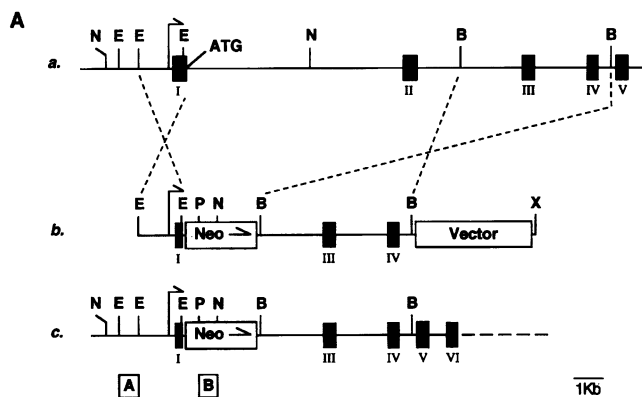


Figure 1. Targeted disruption of the LPL gene. (A) Targeting strategy. Line a represents the map of the LPL genomic DNA containing exons 1–5 (denoted as I–V) (4). The closed boxes and solid lines denote exon sequences and intron or flanking sequences, respectively. Restriction endonuclease sites used for cloning and screening are shown (N, NcoI; E, EcoRI; B, BamHI; P, PstI; X, XbaI). ATG, translation start site. Line b represents the replacement vector *pPW19.1* which contains 1.1 and 5.8 kb of 5' and 3' LPL DNA sequences, respectively, cloned into vector pGKNEO (32). The neomycin resistance gene (*neo*) is driven off the pGK promoter and uses the pGK polyadenylation sequence. Line c illustrates the predicted organization of the LPL locus after homologous recombination. The open boxes A and B represent the flanking and *neo*-specific probes, respectively, used for confirming the targeting event. (B and C) Southern blot analysis of ES cell and mouse tail tip DNA, respectively. DNA was digested with restriction endonuclease NcoI and probed with probe A. Fragment size is reported in kilobases. +/+, normal ES cell and mouse DNA; +/-, targeted ES cell DNA and heterozygous deficient mice; -/-, homozygous deficient mice. (D) Whole-carcass LPL activities. LPL enzyme activity was determined in homogenates of whole carcasses from control ($n = 4$), heterozygous ($n = 12$), and homozygous ($n = 8$) LPL-deficient neonates at 14–16 h after birth. Carcasses were homogenized in DME



Figure 2. Gross pathology in LPL knockout pups at 14–16 h after birth. As compared with controls, LPL knockout pups at 14 h were pale and slightly smaller in size. Over the next 2 h, they became increasingly lethargic and cyanotic, and died. +/+, control pup; -/-, homozygous LPL knockout pup.

(500 mg/kg, i.v.) to block lipolysis (42). Mice were then injected with [^3H] glycerol (100 μCi , i.v.) and blood samples were obtained at 20, 30, 60, 90, and 120 min after glycerol injection. Lipids were extracted according to methods described by Folch (43). Triglycerides were separated by thin-layer chromatography on silica gel G (Analtech Inc., Newark, DE) in hexane/diethyl ether/acetic acid (82:16:1, vol/vol/vol), and radioactivity was determined by liquid scintillation counting.

Vitamin A fat tolerance test. Six control and eight heterozygous mice with serum triglycerides levels of 127 ± 50 and 213 ± 97 mg/dl, respectively, were given intragastric bolus of retinyl palmitate (RP, 3,000 U) in corn oil (100 μl), followed by 150 μl corn oil, followed by 100 μl air. Mice were bled before and 1, 2, 4, and 10 h after vitamin A administration. Retinyl acetate (RA) internal standard was added to serum samples before lipid extraction (44). Samples were resuspended in toluene (15 μl) and analyzed by reverse phase HPLC (Beckman Instruments, Inc., Fullerton, CA) using 2 ml/min methanol as the mobile phase (45). Peak area of RP was normalized to that of RA. To correct for variation in potency of vitamin A batches, results are reported as percentages of maximum RP/RA ratio within each of the two experiments.

Body mass composition analysis of adult heterozygote mice. 4–12-month-old male mice were killed by cervical dislocation and weighed (wet weight). To remove all body water, carcasses were placed in a 90°C convection oven until constant mass was observed. Total water content was calculated as pre-oven carcass weight minus post-oven carcass weight (dry weight). Carcasses were frozen briefly in liquid nitrogen and homogenates were prepared. 1-gram aliquots of homogenate were extracted for 3 h with chloroform/methanol (3:1) in a Soxhlet extraction apparatus with Allihn condenser (Kimble Glass Inc., Vineland, NJ). Extracted samples were weighed to determine lipid content. Total body lipid was calculated as percent lipid in dry carcass multiplied by total dry carcass weight. Lean body mass was calculated as weight before dehydration (wet weight) minus total lipid and water weights. All samples were done in duplicate.

Results

Modification of the LPL gene in ES cells. A replacement vector, *pPW19.1*, was constructed in two cloning steps as shown in

+ 2% BSA and then incubated at 37°C for 1 h in the presence of heparin. LPL activity was measured by methods previously described (37). **P* value (vs. controls) < 0.0005.

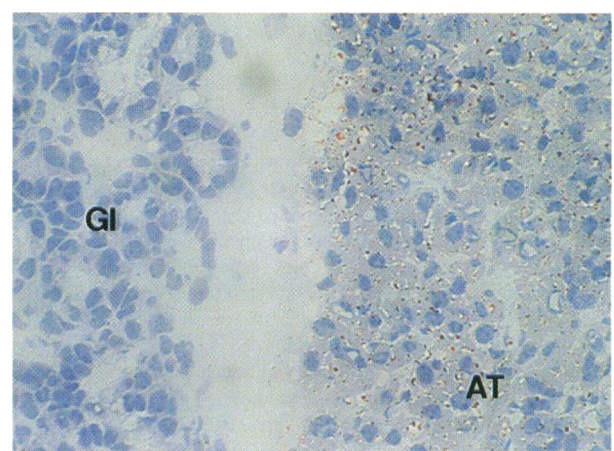
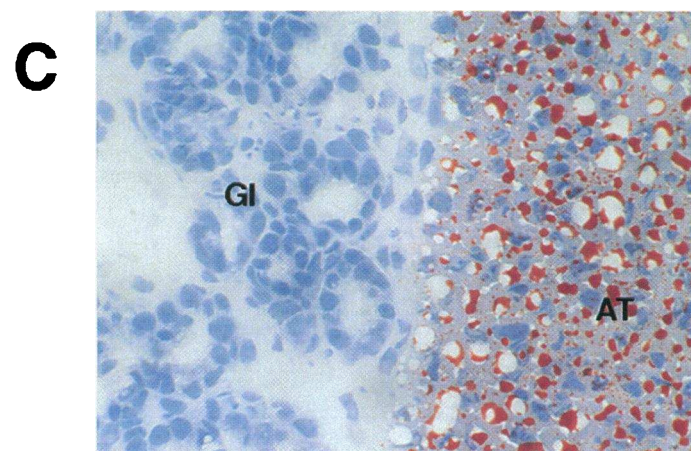
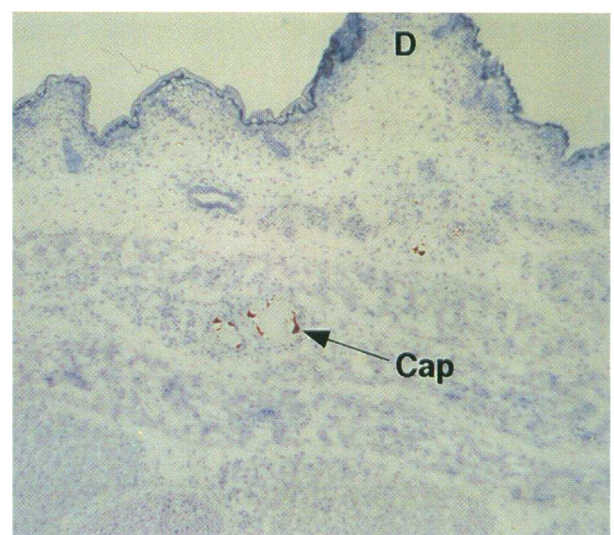
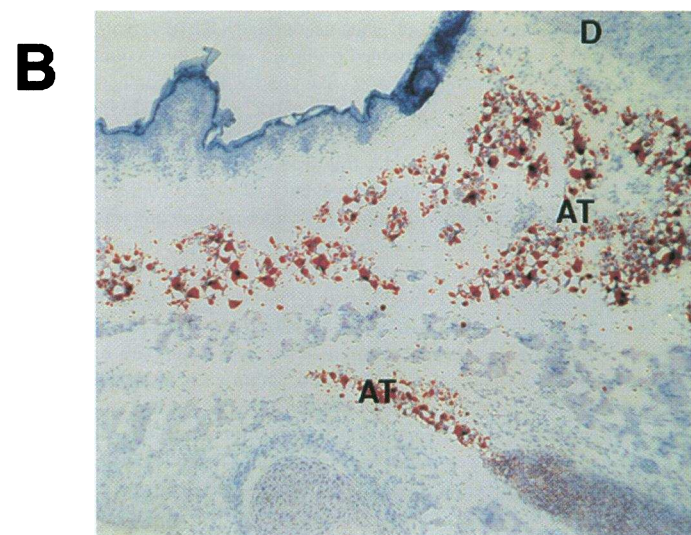
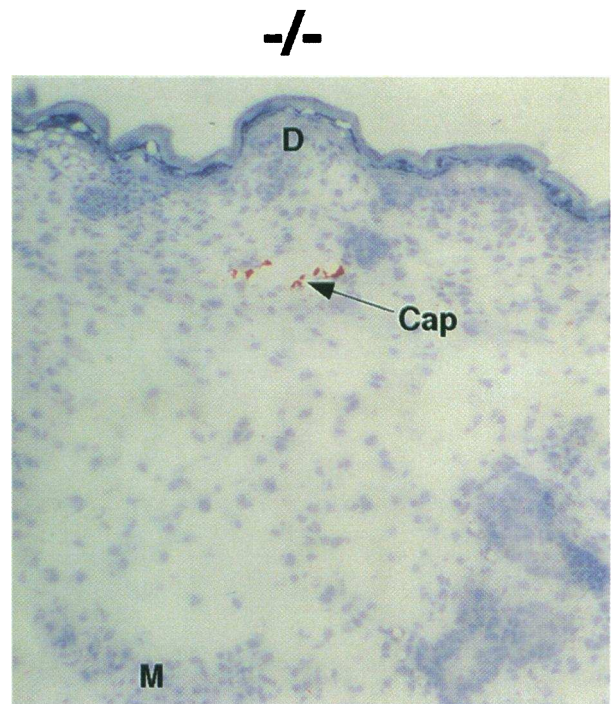
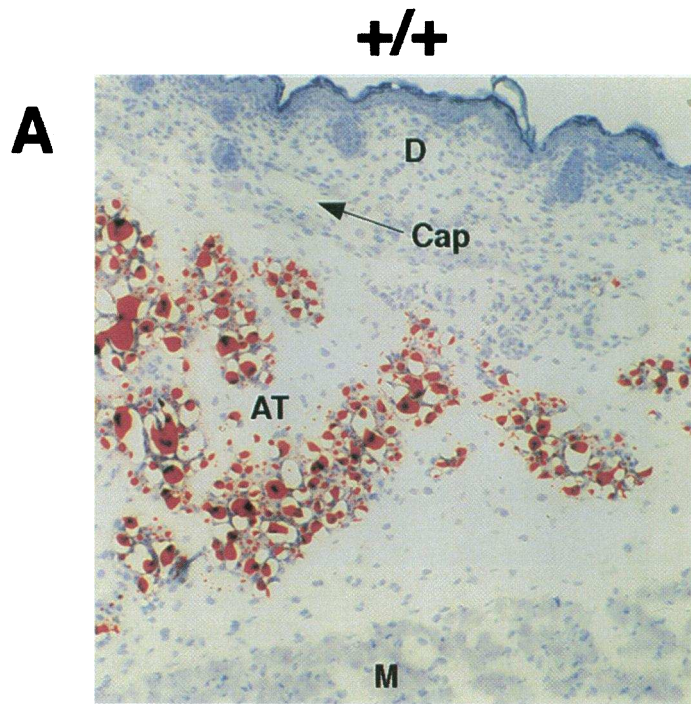


Fig. 1 A. First, a 1.1-kb fragment containing 1 kb of 5' UTR and 100 bp of exon 1 was ligated upstream of the neomycin resistance gene (*neo*) of plasmid *pGKNeo*. A 5.8-kb BamHI fragment containing part of intron 2 through the end of intron 4 was then ligated downstream of *neo*. Homologous recombination between the genomic DNA and the targeting sequences results in a replacement of 8 kb of LPL sequences, including the translation start site and signal sequence of exon 1, intron 1, exon 2, and part of intron 2, with the 1.1-kb *neo* gene. G418-resistant ES cell colonies were expanded and screened by Southern blot to identify those clones that contained the correct modification of the LPL gene and thus had undergone homologous recombination. As shown in Fig. 1 B, hybridization of NcoI-digested ES cell DNA with a 5' 0.7-kb EcoRI DNA fragment (probe A) revealed the endogenous 5.8-kb fragment for wild-type colonies and an additional 3.8-kb fragment in one colony that had undergone the desired homologous recombination event. Probe B for the *neo* gene was used to confirm the positive clone (data not shown).

The positive clone was expanded and injected into 3.5-d-old blastocysts. The 21 mice produced ranged from 5 to 80% chimeric, as determined by agouti contribution to coat color. One mouse (80% chimeric) transmitted the ES cell genome to its progeny. These pups were then screened using the same strategy as for ES cells, and germ line transmission of the LPL mutation was confirmed. Heterozygous mice were interbred, resulting in the correct Mendelian ratio of wild-type (+/+) to heterozygous (+/-) to homozygous knockout (-/-) mice as shown in Fig. 1 C. To confirm that the LPL gene had indeed been knocked out, whole-carcass LPL activity was measured on 16-h-old pups that were genotypically +/+, +/-, and -/- and found to be 0.2, 0.1, and < 0.001 mM free fatty acids liberated/gram of carcass/min, respectively (Fig. 1 D).

Gross and ultrastructural pathology of the LPL knockout mouse. At birth LPL +/+, +/-, and -/- animals appear alike. If allowed to suckle, +/- pups develop normally, as compared with +/+ pups, while -/- pups become progressively pale and then cyanotic, and die by ~16–18 h of age (several animals survived as long as 24 h) (Fig. 2). In the premonitory state (16 h of age), light microscopy reveals widespread pathology. Several adipose tissue storage sites were investigated in multiple animals including subcutaneous adipose tissue (Fig. 3, A and B) and stores near the mandibular salivary glands (Fig. 3 C). While +/+ littermates have significant deposits in all sites investigated, the -/- pups reveal a severe reduction or complete absence of adipose tissue. The livers of +/+ animals contain copious amounts of intracellular lipid droplets, while in the livers of -/- pups these are largely absent (Fig. 4, A–D) with very large amounts of lipid appearing in the sinusoids. Electron microscopy of -/- pup liver revealed extravasation of lipid from the lipid-engorged sinusoids into the intercellular spaces. This appears to have disrupted tight junctions and caused a general breakdown of parenchymal ar-

chitecture (Fig. 4 E). As in the liver, electron microscopy of skeletal muscle from -/- mice reveals a marked reduction of both perinuclear (Fig. 5 A) and perisarclemic (Fig. 5 B) lipid droplets compared with controls. The lungs of -/- animals contain lipid-filled alveoli (not shown) as well as dilated capillaries engorged with large lipoprotein particles (Fig. 6 A). Electron microscopy shows that within capillaries these particles are margined and appear to block contact of the centrally located red blood cells with the endothelium (Fig. 6 B).

Lipoprotein profiles and plasma lipids in mice lacking LPL. HPGC was performed on small volumes of plasma to determine the lipoprotein profiles in +/+, +/-, and -/- pups at 0 and 18 h of age (Fig. 7). At birth the lipoprotein profiles of +/+ and +/- animals were essentially identical and had very small to undetectable VLDL peaks, with the predominance of cholesterol in LDL. In comparison, 0-h profiles from -/- pups revealed a larger VLDL peak with an apparent slight decrease in LDL and HDL. Compared to 0 h, profiles at 18 h for +/+ and +/- pups had increased VLDL with a shift from LDL to HDL predominance. At 18 h, the profile for the -/- pups showed a dramatic increase in VLDL with markedly decreased to undetectable LDL and HDL. Total triglycerides and total and lipoprotein subfraction cholesterol levels were quantitated, with the results shown in Table I. At 0 h, lipid and lipoprotein levels were similar in +/+ and +/- mice. While having normal total cholesterol, -/- mice had a threefold increase in triglycerides and a sevenfold increase in VLDL-C compared with controls. At 18 h, triglycerides had increased in mice with all three genotypes but to a greater extent in the heterozygous and homozygous LPL knockout mice than in controls. Compared with +/+ mice, the +/- mice had a 3-fold increase and the -/- mice a dramatic 80-fold increase in triglyceride levels. Whereas total and lipoprotein cholesterol levels were not different in +/- versus +/+ mice, the -/- mice had elevated total and VLDL-C and diminished LDL-C and HDL-C levels.

Rescue of LPL knockout animals by breeding with transgenic mice expressing LPL exclusively in muscle. LPL is expressed in many tissues in the body, and it was of interest to determine whether the LPL -/- mice could be rescued and the lipoprotein profile normalized by expressing the enzyme in a single tissue. This was done by breeding a transgenic line containing the mouse muscle creatine kinase promoter driving a human LPL minigene onto the LPL knockout background. In a recent study, we showed that the transgene present in this line conferred human LPL expression only in skeletal and cardiac muscle and not in other tissues (46). Muscle-specific expression of LPL rescued the LPL knockout mice, allowing them to survive into adulthood, at which time they had a normal lipoprotein profile as shown in Fig. 8. These results show that LPL expression in a single tissue can rescue the null mice and strongly suggest that neonatal death is due to the LPL deficiency and the resultant hypertriglyceridemia, rather than to a hidden homozygous lethal mutation inadvertently induced in the ES cell clone that gave rise to the LPL knockout mice.

Figure 3. Histological examination of fat stores in control and LPL knockout pups at 16 h of age. (A and B) Light microscopy of oil red O-stained sections from skin covering the right foreleg ($\times 100$) and back ($\times 50$), respectively. Note the severe reduction in subcutaneous adipose tissue in the knockout pup as compared with the control animal. Capillaries are clear in controls and are filled with stained lipid in the knockout pups. (C) Light microscopy of adipose tissue near salivary gland ($\times 400$). Note the copious amounts of large, univacuolar adipocytes in control pups as compared with knockouts, where adipose tissue is severely reduced. +/+, control pup; -/-, homozygous LPL knockout pup; D, dermis; AT, adipose tissue; Cap, capillaries; M, muscle.

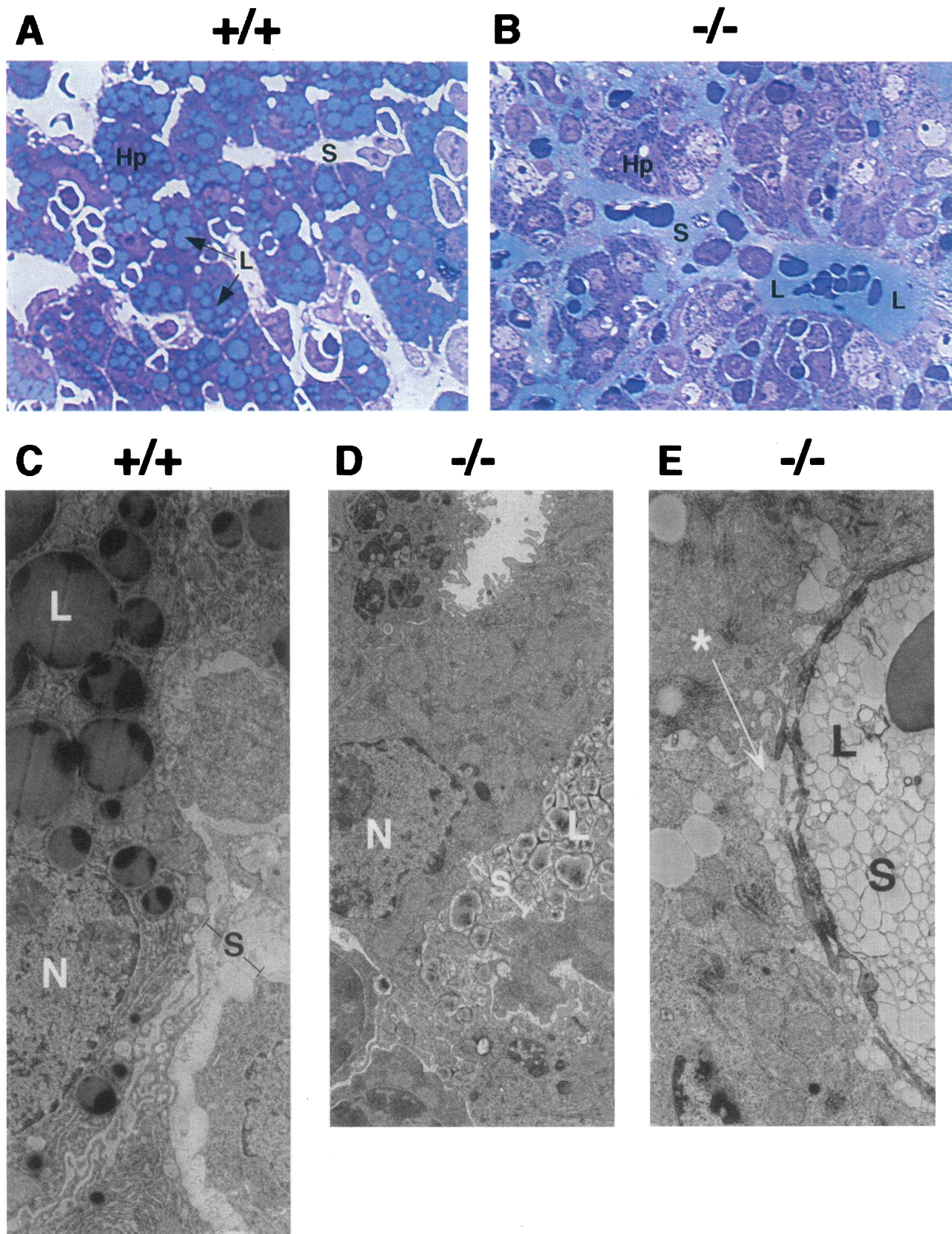


Figure 4. Light and electron microscopy of liver in control and LPL knockout pups at 16 h of age. (A and B) Light microscopy of Epon sections of liver stained with methylene blue/Azure II ($\times 100$) and (C and D) electron microscopy ($\times 8,250$) show numerous intracellular lipid droplets in the control animal, while this lipid appears instead in the sinusoidal space in the knockout. (E) Electron microscopy of $-/-$ pup liver reveals extravasation of lipid (*) from the lipid-engorged sinusoids through endothelial fenestrations into the intercellular spaces ($\times 16,500$). $+/+$, control pup; $-/-$, homozygous LPL knockout pup; Hp, hepatocyte; L, lipid; S, sinusoid; N, nucleus.

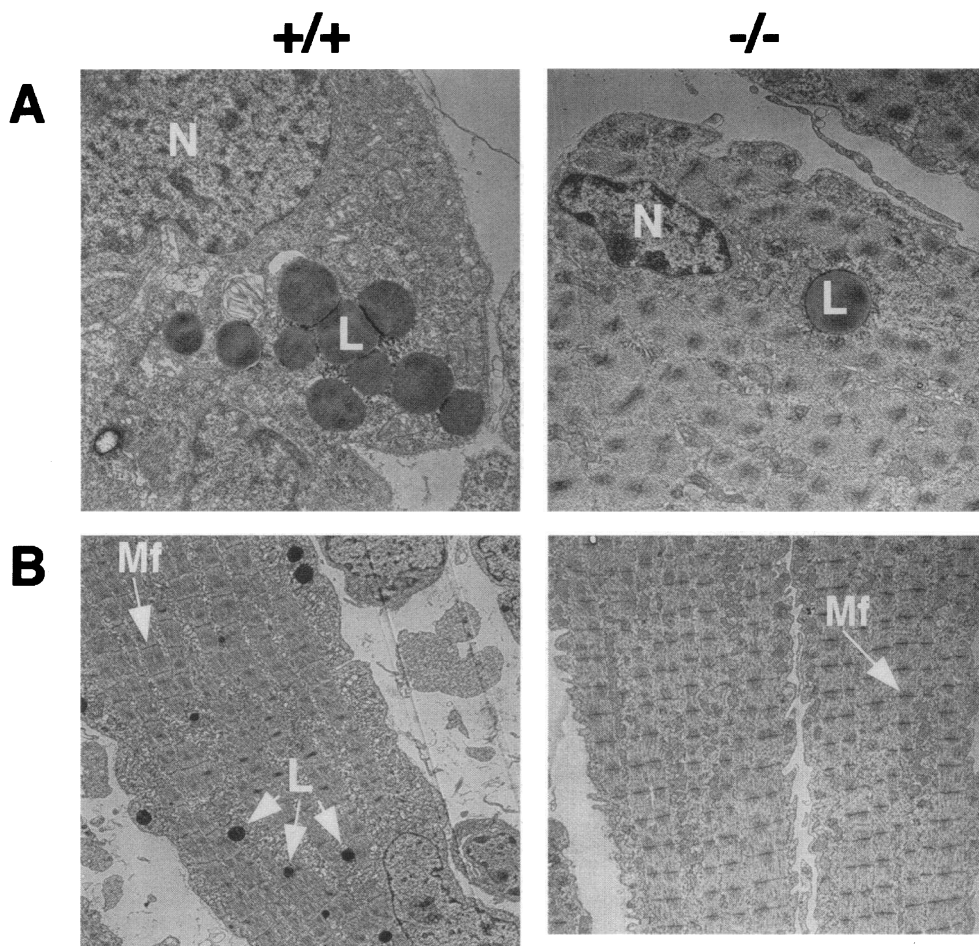


Figure 5. Electron microscopy of skeletal muscle in control and LPL knockout pups at 16 h of age. Note the severe reduction in both perinuclear (A, +/+, $\times 20,750$; -/-, $\times 16,500$) and perisarcoplasmic (B, $\times 8,250$) lipid droplets in the knockout pups as compared with controls. +/+, control pup; -/-, LPL knockout pup. L, lipid; N, nucleus; Mf, myofibrils.

Plasma lipids in adult heterozygous LPL knockout mice. Adult heterozygous LPL knockout mice were used to test the effect of half-normal total body LPL on triglyceride levels. Adult control and +/- mice were fed three types of diets, a low-fat chow diet (9% of calories as long-chain fatty acids), a Western-type diet (40% of calories as long-chain fatty acids), and a chow diet enriched in carbohydrates by supplementation of 10% sucrose in the drinking water. Triglycerides were measured in both the fed and the fasting condition. As shown in Table II, on each diet, in both the fed and fasted states, triglyceride levels were 52–126% higher in the +/- animals compared with controls. Total cholesterol was only modestly elevated (10–30%) in heterozygous knockout mice compared with controls. Lipoprotein subfraction analysis indicated that the increases in triglycerides and cholesterol were in the VLDL fraction as expected, but there was no change in LDL-C or HDL-C levels (data not shown).

VLDL metabolism in heterozygous LPL knockout mice. A VLDL turnover study was performed to determine the metabolic cause of the hypertriglyceridemia observed in the heterozygous LPL knockout mice. VLDL endogenously labeled with [^3H]-palmitate was injected into control and +/- mice and plasma radioactivity was measured over time. As shown in Fig. 9, radioactivity was lost more slowly from heterozygous LPL knockout plasma than from control plasma. This was most impressive during the first 20 min of the decay curve (Fig. 9 A). Clearance of radioactivity from the plasma was consistent with

a two-pool model and the VLDL production rate (PR) considered to be the fractional catabolic rate (FCR) times the pool size. As shown in Table III, there was a 42% reduction in the VLDL FCR in the +/- mice compared with +/+ mice, with no increase in PR. The change in FCR could therefore entirely account for the increase in plasma triglycerides in the heterozygous LPL knockout mice. Furthermore, as shown in Fig. 9 B, triglyceride levels correlate with the VLDL-FCR whether one considers all the mice together or the +/+ and +/- groups separately. A second method was used to confirm that the PR of VLDL in the heterozygous LPL knockout mice was not elevated. Control and +/- mice were treated with Triton WR 1339 to block VLDL clearance, and the time course of incorporation of [^3H]-glycerol into VLDL triglycerides was shown to be the same in these two groups of mice (Fig. 9 C).

Dietary fat clearance in heterozygous LPL knockout mice. A vitamin A fat tolerance test was used to assess dietary fat (chylomicron) clearance in the heterozygous LPL knockout mice. Since hydrolysis of chylomicron triglycerides by LPL is the first step in dietary fat clearance, this test is an appropriate way to assess the adequacy of the enzyme. In the absence of malabsorption, the level of plasma RP over time is inversely proportional to the rate at which chylomicrons are cleared from the circulation. A bolus of RP was administered by oral gastric tube, and plasma levels of RP were measured at 1, 2, 4, and 10 h. Fig. 10 shows that plasma RP levels peaked at 2 h, with the levels in the +/- mice greater than those in the +/+ mice at

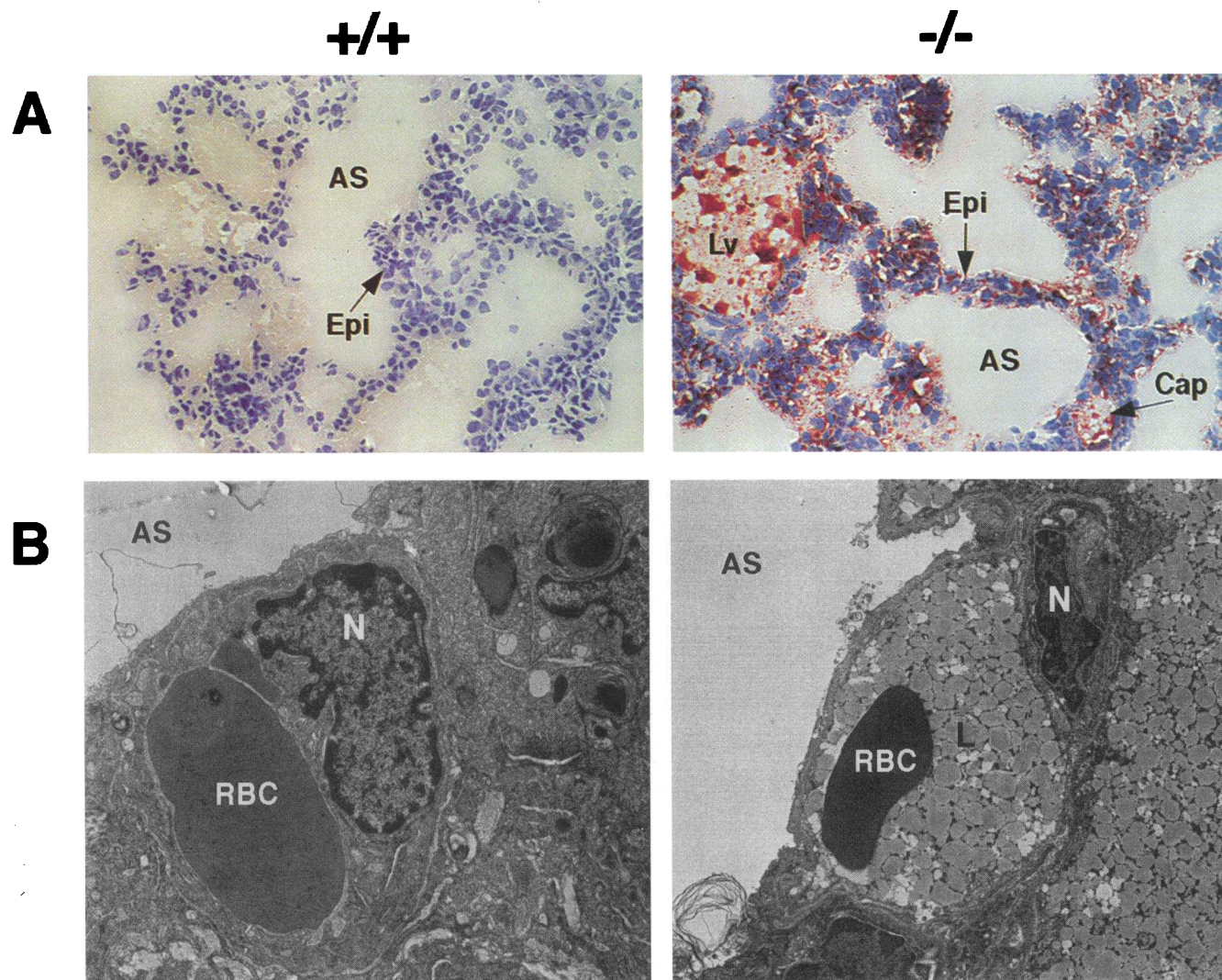


Figure 6. Microscopic examination of lung in control and LPL knockout pups at 16 h of age. (A) Light microscopy of lung. Large vessels as well as small capillaries bounded by alveolar epithelium are filled with lipid in knockout animals while clear in controls ($\times 300$). (B) Electron microscopy of alveolar-capillary junction. Control shows red blood cell in close proximity to capillary endothelium, allowing for proper gas exchange. Note lipid-engorged capillaries in knockout pup, with large lipoproteins surrounding the red blood cell on all sides ($\times 8,250$). +/+, control pup; -/-, LPL knockout pup; AS, alveolar space; Lv, large vessel; Epi, alveolar epithelium (pneumocytes); Cap, capillary; L, lipoproteins; N, nucleus of capillary endothelial cell; RBC, red blood cell.

1, 2, and 4 h. Thus, there was a delay in clearance of chylomicrons as well as VLDL in the heterozygous LPL knockout mice.

Body mass composition analysis of adult heterozygous LPL-deficient mice. To determine whether a 50% reduction in whole-body LPL is associated with alterations in body mass composition, in particular decreases in adipose tissue mass, body mass composition analysis was performed on both 129/b6 and 129 strain heterozygote mice. Table IV demonstrates that mice ranging in age from 4 to 8 mo (129/b6 strain, experiment 1) and as old as 12 mo (129 strain, experiment 2) are of normal weight and have normal amounts of water, lipid, and lean body mass. In addition, quantitative histological analysis of abdominal fat stores from these mice showed equal amounts of adipose tissue at all sites observed (data not shown).

Discussion

Knocking out the LPL gene in the mouse has led to several dramatic findings, including the requirement of LPL for sur-

vival, adipose tissue development, and entry of fat into many tissues, including liver and muscle. These observations were unexpected, since type I hyperlipoproteinemia (homozygous LPL deficiency) is not generally lethal, nor has it been reported to be associated with obvious abnormalities in adipose tissue development or body composition, even in patients who have no measurable LPL enzymatic activity (47). There are several possible explanations for the differences in phenotype between LPL-deficient mice and humans. The first is that we have introduced a null mutation into the mice, whereas most of the human mutations are of the missense variety (48). It may be that small amounts of activity not measurable by the standard assay exist in type I humans or that structural features of LPL such as its postulated bridging function, rather than its enzymatic activity, are required for survival. Secondly, rodent milk is higher in fat (12.3 grams/100 ml) than human milk (4.0 grams/100 ml) and rodents ingest more calories per gram than humans (49). Thus, the neonatal fat load in mice is greater than in humans.

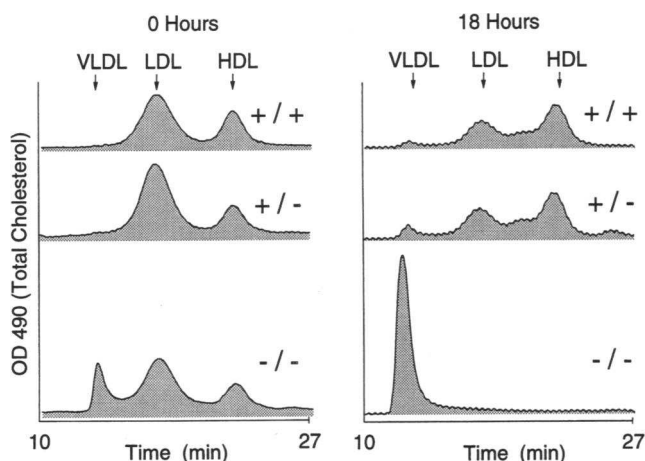


Figure 7. Lipoprotein total cholesterol profile by HPGC in 0-h (before suckling) and 18-h-suckled pups. Total lipoprotein cholesterol profiles were determined by on-line post-column analysis of Superose-6 gel-filtered mouse serum (2.5–10 μ l). Plasmas from pups killed and bled at 0 h (before suckling) and after 18 h of suckling (before death) were analyzed. These analyses were performed on a Beckman Gold system. Lipoprotein cholesterol distribution was determined from percent area distribution in profiles and from independent determinations (in whole serum). All profiles are in the same scale. Table I summarizes lipoprotein triglyceride and cholesterol data from all mice. Lipoprotein peaks are labeled above each set of profiles (VLDL, LDL, and HDL, respectively). +/+, control; +/-, heterozygote; -/-, homozygote LPL-deficient pup.

When LPL is deficient, this may result in more severe hypertriglyceridemia in newborn mice compared with human neonates. Thirdly, we have determined that the sharp rise in plasma triglycerides observed in LPL-deficient mice after suckling is due to the fact that virtually all of the ingested fat remains in plasma. Thus, in the mouse it appears that the only route of plasma triglyceride removal is via LPL. This may not be true for humans, as significant differences exist between the lipoprotein systems of the two species which could affect triglyceride removal. For example, there are considerable differences between rodents and humans in hepatic lipase, which normally does not hydrolyze significant amounts of triglyceride in chylomicrons and VLDL. In the mouse, hepatic lipase circulates in the plasma whereas in humans it resides in the liver (50). In LPL defi-

ciency, liver-bound hepatic lipase may hydrolyze chylomicron and VLDL triglycerides better than circulating hepatic lipase, providing partial compensation for LPL deficiency in humans but not in mice. In addition, amino acid differences exist between rodent and human hepatic lipase which could alter substrate specificity enough to allow for some chylomicron and VLDL triglyceride hydrolysis by the human enzyme (51, 52). Another possibility is that the lack of cholesterol ester transfer protein in the mouse may prevent the transfer of triglycerides to HDL, precluding triglyceride hydrolysis by hepatic lipase. Other mechanisms may also exist in humans which allow LPL-independent plasma triglyceride removal, such as increased numbers or increased affinities of lipoprotein receptors for triglyceride-rich lipoproteins such as the VLDL receptor (53, 54). At this point, we cannot distinguish among these possibilities. However, through altering the diet of the newborn mouse or crossbreeding various transgenes onto the LPL knockout background, some of these hypotheses can be tested.

Histopathologic analysis of the LPL knockout mice just before death reveals dilated capillaries that are engorged with chylomicrons in many tissues. In the lung, these large particles are margined and appear to block contact between red blood cells and the endothelium. This probably prevents efficient gas exchange and results in a ventilation-perfusion abnormality leading to cyanosis and death. The severe hyperchylomicronemia may also increase blood viscosity, further impeding normal blood flow and tissue perfusion. Alveolar lipid is observed in the lungs of -/- pups (not shown) and is most likely the result of alveolar damage caused by capillary occlusion and hemorrhage. The fact that the lungs of -/- pups also contain generous amounts of lipid-laden intraalveolar macrophages (while +/+ and +/- pups do not), as well as intact lipid-filled pneumocytes which line the alveoli, confirms that the accumulation of alveolar lipid is a real pathophysiological process in these animals rather than an artifact of tissue preparation. Similar findings have also been reported in combined lipase-deficient mice (*clid*) (8). These animals have a defect in a gene, distinct from the structural gene for each of these enzymes, that controls the intracellular processing of both LPL and hepatic lipase. The *clid* mice produce inactive, nonsecretable forms of both enzymes and develop severe hypertriglyceridemia after birth (9). They survive slightly longer than the LPL knockout mice but expire at 2–3 d of age. The pathologic picture in the lung is similar to the LPL knockout mice and a similar cause

Table I. Plasma Cholesterol and Triglyceride Levels in LPL-deficient Pups

Time	Strain	Genotype	n	Triglycerides	Cholesterol			
					Total	VLDL	LDL	HDL
					<i>mg/dl</i>			
0	129/B6	+/+	5	30 \pm 7	55 \pm 13	1.2 \pm 0.1	40 \pm 13	14 \pm 3
0	129/B6	+/-	13	45 \pm 13	59 \pm 11	2.2 \pm 1.7	41 \pm 11	14 \pm 2
0	129/B6	-/-	7	93 \pm 26*	51 \pm 9	8.2 \pm 3.1*	30 \pm 7	11 \pm 3
18	129/B6	+/+	4	188 \pm 71 [‡]	57 \pm 9	6 \pm 4 [§]	21 \pm 3 [§]	31 \pm 8 [‡]
18	129/B6	+/-	6	568 \pm 377	80 \pm 21 [‡]	10 \pm 5	40 \pm 16	28 \pm 6
18	129/B6	-/-	12	15087 \pm 3805*	288 \pm 9*	280 \pm 92*	7 \pm 4*	4 \pm 3*

* *P* value (vs. +/+ littermate of same age) < 0.001; [§] *P* value (vs. same genotype at 0 h) < 0.04; [‡] *P* value (vs. same genotype at 0 h) < 0.01; ^{||} *P* value (vs. same genotype at 0 h) < 0.001.

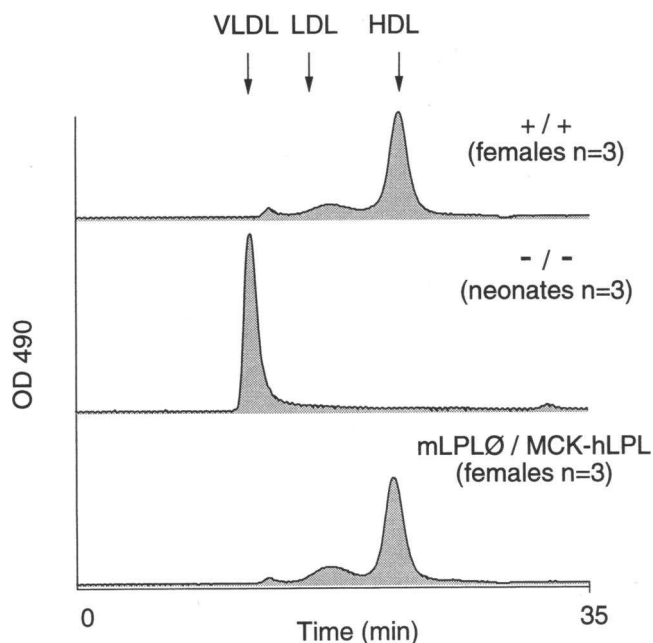


Figure 8. Muscle-specific expression of human LPL rescues LPL-deficient mice. Control (+/+) pups, knockout (-/-) pups, and pups expressing the human LPL transgene in skeletal muscle only (mLPL0/MCK-hLPL strain) were killed at 16 h and plasma was obtained for cholesterol measurement. Animals were bled and total cholesterol profiles were performed as described earlier.

of death has been postulated. It was previously thought that the severity of the phenotype in the *cld* mouse was due to the combined lipase deficiency. However, this now appears not to be the case, since isolated LPL deficiency can cause death at an even earlier age. The severity of the LPL defect and the resulting hypertriglyceridemia are probably sufficient to account for the deaths of both the LPL knockout and the *cld* mice. Further evidence that it is the hypertriglyceridemia that kills the mice is provided by the rescue of the LPL knockout mice by a muscle-specific human LPL transgene (46). This rescue also demonstrates that LPL expression in a single tissue is sufficient to normalize the lipoprotein pattern and that LPL expression in other tissues of the body (i.e., adipose tissue, brain, macrophages, etc.) is not necessary for survival. Generating

these animals has also established feasibility for future experiments addressing physiological effects of LPL activity at various organs on the otherwise null background.

The LPL-deficient pups fail to develop normal amounts of adipose tissue. This is especially apparent in the subdermal skin layer and is presumably due to an inability to hydrolyze triglycerides in adipose tissue capillary endothelium, preventing the transport of free fatty acids into adipocytes. These animals provide direct evidence that LPL is required for the entry of triglyceride-derived free fatty acids into adipose tissue. In addition, the LPL knockout mice also had severely depleted intracellular lipid in other tissues, such as liver and skeletal muscle, supporting the hypothesis that LPL serves as the predominant gatekeeper for the import of fat into all tissues. Greenwood (23) observed inappropriate overactivity of LPL in several models of animal obesity, as well as in human obesity, and postulated that this caused an increase in adipose tissue mass. Based on these studies, Greenwood postulated a role for LPL in the development of obesity (24). According to this theory, increased LPL activity in adipose tissue could lead to enhanced adipose storage of fat-derived calories, and perhaps caloric deficiency in other tissues might lead to increased caloric intake as well. Thus it appears that both complete absence as well as overexpression of adipose tissue LPL can affect the amount of adipose tissue, yet moderate decreases in whole body LPL, as seen in heterozygote mice, are not enough to produce these effects as these mice reveal normal body mass composition and, in particular, normal body lipid content.

The lipoprotein patterns of the LPL knockout mice at 0 and 18 h of age have some unusual features. At 0 h, triglycerides are mildly increased and HDL-C levels are not significantly diminished compared with controls. LPL had been thought to play a crucial role in the assembly of HDL particles due to the transfer of excess surface constituents from VLDL to HDL during triglyceride hydrolysis (5). LPL activity in post-heparin plasma has been correlated with circulating levels of HDL in humans (55, 56). Moreover, inhibition of LPL in monkeys produced a rapid decrease in circulating HDL levels and increased the rate of catabolism of apo A-I (57), the major protein component of HDL. The existence of normal levels of HDL in newborn LPL knockout mice demonstrates that at least some HDL can be formed in the absence of LPL. At 18 h, triglycerides are severely elevated and HDL-C levels are very low to absent in LPL knockout mice. In humans with type I hyperlipoproteinemia, this pattern is expected because of the exchange of triglyc-

Table II. Plasma Triglycerides of Heterozygote LPL-deficient Adult Mice

Genotype	Triglycerides (mg/dl)					
	Chow		WTD		10% sucrose	
	Fed	Fasted	Fed	Fasted	Fed	Fasted
+/+	177±13 (n = 4)	52±15 (n = 4)	187±70 (n = 7)	82±18 (n = 7)	112±56 (n = 7)	76±23 (n = 7)
+/-	270±54 (n = 9)	118±21 (n = 9)	351±74 (n = 8)	130±25 (n = 8)	177±51 (n = 6)	153±58 (n = 6)
<i>P</i> value <	0.01	0.001	0.001	0.001	0.05	0.01

Data are means + standard deviation. WTD, Western-type diet.

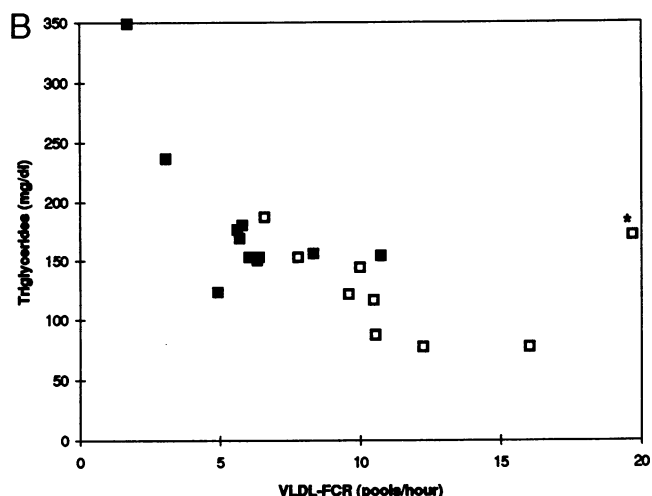
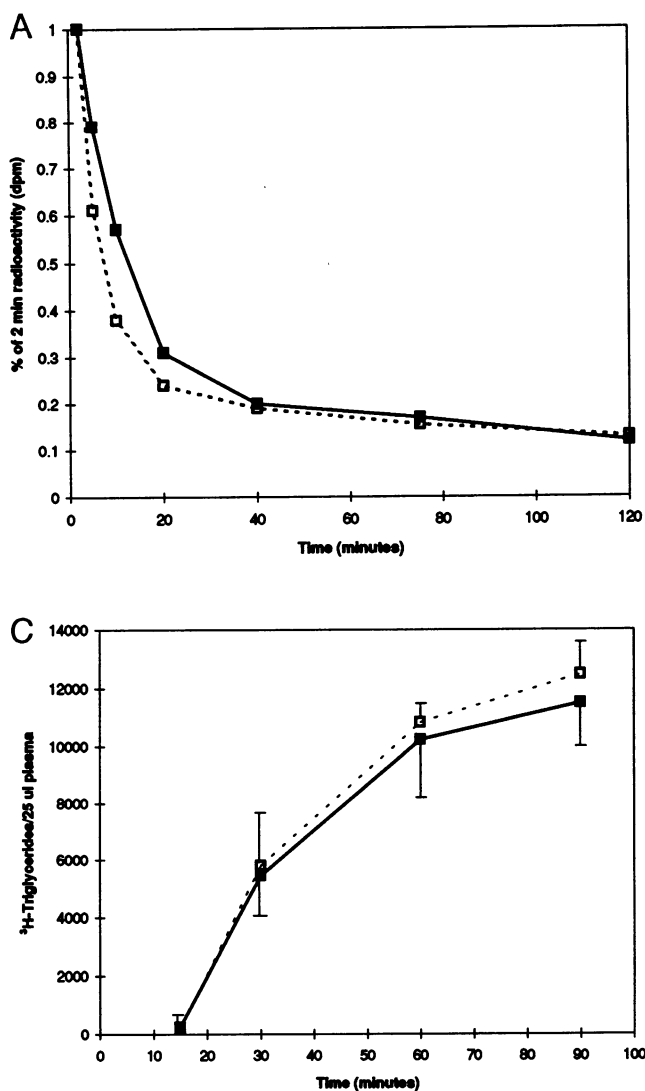


Figure 9. VLDL triglyceride clearance and production in LPL heterozygote mice. VLDL clearance was studied in 10 control (*open boxes*) and 10 heterozygote (*closed boxes*) mice using ^3H -triglyceride VLDL metabolically labeled in control mice as described in Methods. ^3H -triglyceride VLDL was intravenously administered to mice and serum radioactivity was determined at intervals up to 120 min. (A) Typical radioactive decay curves for ^3H -labeled VLDL triglycerides in control and LPL heterozygote mice. (B) Plasma triglyceride levels as a function of VLDL-FCR. R^2 values for $+/+$ animals (*open boxes*) analyzed with and without the outlier (*) were 0.74 ($P < 0.003$) and 0.07, respectively. R^2 value for $+/-$ (*closed boxes*) animals was 0.48 ($P < 0.03$). R^2 values for both $+/+$ and $+/-$ groups combined were 0.34 ($P < 0.007$) with, and 0.64 ($P < 0.0001$) without the outlier. Data from all mice studied were used to determine triglyceride fractional catabolic and production rates and are shown in Table III. (C) Hepatic triglyceride production was determined in three control (*open boxes*) and three LPL heterozygote deficient (*closed boxes*) mice as described in Methods. Mice were treated with Triton WR 1339 (to block lipolysis) and then intravenously injected with [^3H]-glycerol. Serum triglyceride radioactivity was determined up to 2 h after injection. Data represent mean + standard deviation.

erides for HDL cholesterol esters mediated by cholesterol ester transfer protein, a process which facilitates hepatic lipase hydrolysis of HDL triglycerides, causing a decrease in the size of the HDL particle and an increased apo A-I FCR (58). The mouse, however, is deficient in cholesterol ester transfer protein, as noted previously, and might not be expected to show such a severe decrease in HDL-C levels. In a previous hypertriglyceridemia model, the apo CIII transgenic mouse, we also observed

Table III. VLDL Triglyceride FCRs and PRs for Control and LPL Heterozygote Mice

Genotype	n	Weight	TG	FCR	PR
		grams	mg/dl	pools/h	pools/h
$+/+$	10	28.0 ± 1.8	129 ± 39	10.9 ± 4.2	0.45 ± 0.24
$+/-$	10	26.9 ± 3.3	185 ± 65	5.8 ± 2.5	0.32 ± 0.11
$P <$		NS	0.03	0.004	NS

Data are means + standard deviation. TG, triglyceride.

decreased HDL-C in the face of hypertriglyceridemia and found a decrease in the apo A-I synthetic rate in part due to a decreased level of intestinal apo A-I mRNA levels (42, 59). Although this cannot be studied in premonitory 18-h-old LPL-deficient mice, it may be that the hypertriglyceridemia is limiting apo A-I production, as we observed in the previous model.

Heterozygous LPL-deficient mice exhibit moderate hypertriglyceridemia in both the fed and fasted state on several diets. The largest effect was seen in the fed state with the mice on the high-fat Western-type diet. Metabolic studies in heterozygous LPL-deficient mice indicated that the hypertriglyceridemia was caused by decreased catabolism of triglyceride-rich lipoproteins rather than by increased production. If the amount of LPL in the body was in great excess this would not have occurred, suggesting that LPL is rate limiting in normal triglyceride metabolism. One might expect this to be even more evident at times of stress, which may increase the production of triglyceride-rich lipoproteins (10–14). These observations strongly reinforce observations in humans, where because of potential confounding variables it has been difficult to be certain that there is a cause and effect relationship between moderate increases or decreases in LPL levels and plasma triglycerides. For example,

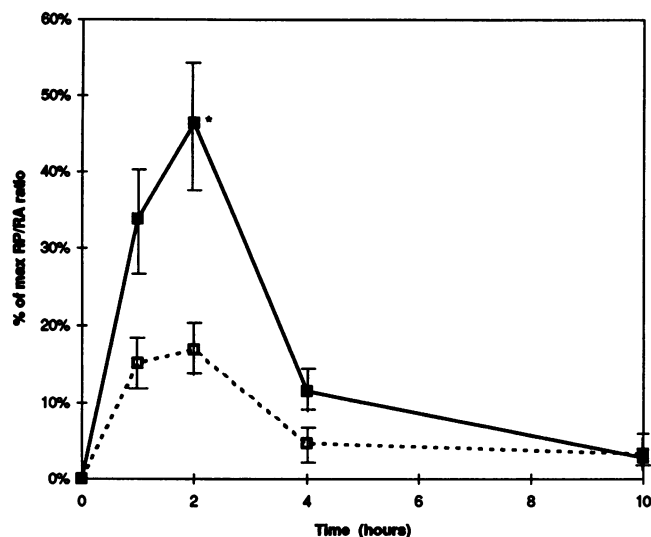


Figure 10. Vitamin A fat tolerance in LPL heterozygote mice. Intestinal absorption and clearance of RP was assessed in six control (open boxes) and eight heterozygote (closed boxes) mice as described in Methods. At intervals up to 10 h, mice were bled, and serum RP content relative to RA (internal standard) was determined. * $P < 0.05$. Data represent mean + standard error.

while in hypertriglyceridemic diabetics it has been suggested that the amount of LPL is inadequate (60), other explanations are possible, including increased production of triglyceride-rich lipoproteins or decreased catabolism due to overproduction of apo CIII (42). In another example, heterozygote relatives of type I hyperlipoproteinemic probands tend to be hypertriglyceridemic, but this is associated with confounding variables such as advancing age and other risk factors for hypertriglyceridemia, including adiposity and glucose intolerance (14). The observations reported here in the heterozygous LPL-deficient mouse indicate that a primary deficiency in the LPL gene causing half-normal total body LPL is sufficient to cause a significant alteration in triglyceride-rich lipoprotein catabolism resulting in hypertriglyceridemia.

In addition to hypertriglyceridemia, heterozygous LPL deficiency has been postulated to play a role in a more complex

dyslipoproteinemia phenotype, FCHL (15–17). This disorder has been postulated to be monogenic and is characterized by increased VLDL and/or LDL levels in affected family members (61). Metabolically, the main feature appears to be increased production of VLDL apo B by the liver. Williams (62) has shown in vitro that LPL can increase the reuptake of nascent VLDL by the hepatocyte. He postulates that LPL serves to remodel newly formed lipoproteins in the space of Disse, promoting their immediate reuptake by the cell, and that partial LPL deficiency, as seen in heterozygotes for LPL mutations, may cause increased VLDL production in vivo. Consistent with this theory, Brunzell (15) has described a subset of individuals with FCHL who have a reduced LPL activity-to-mass ratio similar to what one would expect in individuals with heterozygous LPL deficiency, producing an active enzyme from one allele and an inactive enzyme from the other. However, DNA sequencing failed to reveal significant LPL gene structural mutations in these subjects (16). In heterozygous LPL knockout mice, VLDL turnover studies as well as more direct measurements of VLDL production in Triton-treated animals failed to show evidence for increased VLDL production in vivo. Our findings in the mouse suggest that primary LPL deficiency probably does not underlie the increased VLDL apo B production observed in patients with FCHL. Our findings, together with those of Brunzell, suggest that as yet unknown mechanisms may regulate LPL activity.

In summary, LPL-deficient mice have extended our knowledge of the role of this enzyme in the body. In the mouse, it appears that LPL is required for triglyceride removal from the circulation and is a regulator of adipocyte development and intracellular lipid stores. These observations were unexpected in view of the features of type I hyperlipoproteinemic humans, and careful evaluation of the differences between these two phenotypes should provide novel insights into fat transport and energy metabolism. We have also shown that the offspring of LPL-deficient mice crossed with tissue-specific LPL transgenic mice are viable, such mice provide an opportunity to study the effects of expression of LPL in various tissues on plasma lipoproteins as well as energy metabolism. Finally, the studies in heterozygous LPL knockout mice confirm that LPL is rate limiting in the catabolism of triglyceride-rich lipoproteins, but that LPL deficiency is probably not a cause of the increased VLDL apo B production seen in patients with FCHL.

Table IV. Body Mass Composition of LPL Heterozygotes

Genotype	Strain	n	Weight grams	Water		Lipid		LBM	
				Total grams	%*	Total grams	%	Total grams	%
Experiment 1									
+/+	129/b6 [‡]	6	30.0±2.7	19.5±1.0	63±3	3.6±1.5	11±4	7.9±0.5	25±1
+/-	129/b6	8	31.1±2.2	18.6±1.2	60±4	4.8±1.6	15±5	7.6±3.5	25±1
	P value		NS	NS	NS	NS	NS	NS	NS
Experiment 2									
+/+	129 [§]	3	33.1±3.0	20.4±1.6	62±2	5.2±1.0	15±2	7.6±0.6	23±1
+/-	129	5	29.7±2.9	18.3±1.4	62±2	4.0±1.3	13±3	7.4±0.6	25±1
	P value		NS	NS	NS	NS	NS	NS	NS

* Percentage of total weight; [‡] 4–8-mo-old males; [§] 12-mo-old males. LBM, lean body mass.

Acknowledgments

The authors wish to thank Dr. A. S. Plump for his help with ES cells, the Rockefeller Transgenic Service Laboratory (Dr. A. Walsh, Director) for its invaluable help with blastocyst injection, Mr. P. Sheiffelle, Ms. Y. T. Tsang, A. Strudel, and A. Fuchsichler for their expert technical assistance, and Dr. Marilyn Dammerman for her careful review of the manuscript.

References

1. Olivecrona, T., and G. Bengtsson-Olivecrona. 1987. Lipoprotein lipase from milk—the model enzyme in lipoprotein lipase research. In *Lipoprotein Lipase*. J. Borenstajin, editor. Evener, Chicago. 15–25.
2. Olivecrona, T., and G. Bengtsson-Olivecrona. 1993. Lipoprotein lipase and hepatic lipase. *Curr. Opin. Lipidol.* 4:187–196.
3. Wion, K. L., T. G. Kirchgessner, A. J. Lusic, M. C. Schotz, and R. M. Lawn. 1987. Human lipoprotein lipase: complimentary DNA sequence. *Science (Wash. DC)*. 235:1638–1641.
4. Zechner, R., C. Newman, E. Steiner, and J. L. Breslow. 1991. The structure of the mouse lipoprotein lipase gene: a B1 repetitive element is inserted into the 3' untranslated region of the mRNA. *Genomics*. 11:62–76.
5. Eisenberg, S. 1984. High density lipoprotein metabolism. *J. Lipid Res.* 25:1017–1058.
6. Brunzell, J. D. 1995. Familial lipoprotein lipase deficiency and other causes of chylomicronemia syndromes. In *The Metabolic Basis of Inherited Disease*. R. S. Scriver, A. L. Beaudet, W. S. Sly, and D. Valli, editors. McGraw Hill, New York. 1913–1932.
7. Goldberg, I. J., N.-A. Le, H. N. Ginsberg, R. M. Krauss, and F. T. Lindgren. 1988. Lipoprotein metabolism during acute inhibition of lipoprotein lipase in the cynomolgus monkey. *J. Clin. Invest.* 81:561–568.
8. Paterniti, J. R., Jr., W. V. Brown, H. N. Ginsberg, and K. Artzt. 1983. Combined lipase deficiency (cld): a lethal mutation on chromosome 17 of the mouse. *Science (Wash. DC)*. 221:167–169.
9. Masuno, H., E. J. Blanchette-Mackie, S. S. Chernick, and R. O. Scow. 1990. Synthesis of inactive nonsecretable high mannose-type lipoprotein lipase by cultured brown adipocytes of combined lipase deficient cld/cld mice. *J. Biol. Chem.* 265:1628–1638.
10. Harlan, W. R., Jr., P. S. Winesett, and A. J. Wasserman. 1967. Tissue lipoprotein lipase in normal individuals and individuals with exogenous hypertriglyceridemia and relationship of the enzyme to accumulation of fat. *J. Clin. Invest.* 46:239–247.
11. Miesenbock, G., B. Holz, B. Foger, E. Brandstatter, B. Paulweber, F. Sandhofer, and J. Patsch. 1993. Heterozygous lipoprotein lipase deficiency due to a missense mutation as the cause of impaired triglyceride tolerance with multiple lipoprotein abnormalities. *J. Clin. Invest.* 91:448–455.
12. Wilson, D., M. Emi, P. Iverius, A. Hata, L. Wu, E. Hillas, R. Williams, and J. Lalouel. 1990. Phenotypic expression of heterozygous lipoprotein lipase deficiency in the extended pedigree of a proband homozygous for a missense mutation. *J. Clin. Invest.* 86:735–750.
13. Ma, Y., M. S. Liu, D. Ginzinger, J. Frohlick, J. D. Brunzell, and M. R. Hayden. 1993. Gene environment interaction in the conversion of a mild-to-severe phenotype in a patient homozygous for a ser 172-cys mutation in the lipoprotein lipase gene. *J. Clin. Invest.* 91:1953–1958.
14. Williams, R. R., P. Hopkins, S. C. Hunt, M. C. Schumacher, S. C. Elbein, D. E. Wilson, B. M. Stults, L. L. Wu, S. J. Hasstedt, and J. M. Lalouel. 1992. Familial dyslipidemic hypertension and other multiple metabolic syndromes. *Ann. Med.* 24:469–475.
15. Babirak, S., G. Brown, and J. D. Brunzell. 1992. Familial combined hyperlipidemia and abnormal lipoprotein lipase. *Arterioscler. Thromb.* 12:1176–1183.
16. Gagne, E., J. Genest, H. Zhang, L. Clarke, and M. Hayden. 1994. Analysis of DNA changes in the LPL gene in patients with familial combined hyperlipidemia. *Arterioscler. Thromb.* 14:1250–1257.
17. Nevin, D., J. D. Brunzell, and S. Deeb. 1994. The LPL gene in individuals with familial combined hyperlipidemia and decreased LPL activity. *Arterioscler. Thromb.* 14:869–873.
18. Shimada, M., H. Shimano, T. Gotoda, K. Yamamoto, M. Kawamura, T. Inaba, Y. Yazaki, and N. Yamada. 1993. Overexpression of human lipoprotein lipase in transgenic mice. *J. Biol. Chem.* 268:17924–17929.
19. Liu, M., F. Jirik, R. LeBoeuf, H. Henderson, L. Castellani, A. Lusic, Y. Ma, I. Forsythe, H. Zhang, E. Kirk, J. D. Brunzell, and M. Hayden. 1994. Alteration of lipid profiles in plasma of transgenic mice expressing lipoprotein lipase. *J. Biol. Chem.* 269:11417–11424.
20. Zsigmond, E., E. Scheffler, T. Forte, R. Potenz, W. Wu, and L. Chan. 1994. Transgenic mice expressing human lipoprotein lipase driven by the mouse metallothionein promoter. *J. Biol. Chem.* 269:18757–18766.
21. Gruen, R., E. Hietanen, and M. R. C. Greenwood. 1979. Increased adipose tissue LPL activity during the development of the genetically obese rat (fa/fa). *Metab. Clin. Exp.* 27:1955–1966.
22. Eckel, R. 1987. Adipose tissue lipoprotein lipase. In *Lipoprotein Lipase*. J. Borenstajin, editor. Evener, Chicago. 79–132.
23. Greenwood, M. R. C. 1984. Enzymatic alterations in the obese: long and short term regulatory errors? *Int. J. Obes.* 8:561–569.
24. Greenwood, M. R. C. 1985. The relationship of enzyme activity to feeding behavior in rats: lipoprotein lipase as the metabolic gatekeeper. *Int. J. Obes.* 9(Suppl. 1):67–70.
25. Eisenberg, S., E. Sehayek, T. Olivecrona, and I. Vlodavsky. 1992. Lipoprotein lipase enhances binding of lipoproteins to heparan sulfate on cell surface and extracellular matrix. *J. Clin. Invest.* 90:2013–2021.
26. Saxena, U., M. G. Klein, T. M. Vanni, and I. J. Goldberg. 1992. Lipoprotein lipase increases low density lipoprotein (LDL) retention by subendothelial cell matrix. *J. Clin. Invest.* 89:373–380.
27. Nordestgaard, B. G., A. Tybjaerdt-Hansen, and B. Lewis. 1992. Influx in vivo of low density, intermediate density, and very low density lipoproteins into aortic intimas of genetically hyperlipidemic rabbits. *Arterioscler. Thromb.* 12:6–18.
28. Renier, G., E. Skamene, J. B. De Sanctis, and D. Radzioch. 1993. High macrophage lipoprotein lipase expression and secretion are associated in inbred murine strains with susceptibility to atherosclerosis. *Arterioscler. Thromb.* 13:190–196.
29. Rutledge, J. C., and I. J. Goldberg. 1994. Lipoprotein lipase affects low density lipoprotein flux through the vascular wall: evidence that LPL increases LDL accumulation in the vascular wall. *J. Lipid Res.* 35:1152–1160.
30. Schwenke, D. C., and T. E. Carew. 1989. Initiation of atherosclerotic lesion in cholesterol-fed rabbits. II. Selective retention of LDL vs. selective increases in LDL permeability in susceptible sites of arteries. *Arteriosclerosis*. 9:908–918.
31. Traber, M. G., T. Olivecrona, and H. J. Kayden. 1985. Bovine milk lipoprotein lipase transfers tocopherol to human fibroblasts during triglyceride hydrolysis in vitro. *J. Clin. Invest.* 75:1729–1734.
32. Rudnicki, M. A., T. Braun, S. Hinuma, and R. Jaenisch. 1992. Inactivation of MyoD in mice leads to upregulation of the myogenic HLH gene Myf-5 and results in apparently normal muscle development. *Cell*. 71:383–390.
33. Li, E., T. H. Bestor, and R. Jaenisch. 1992. Target mutation of the DNA methyltransferase gene results in embryonic lethality. *Cell*. 69:915–926.
34. Robertson, E. J. 1987. Embryo-derived stem cells. In *Teratocarcinomas and Embryonic Stem Cells: A Practical Approach*. E. J. Robertson, editor. Oxford/IRL Press. 71–112.
35. Bradley, A. 1987. Production and analysis of chimeric mice. In *Teratocarcinomas and Embryonic Stem Cells: A Practical Approach*. E. J. Robertson, editor. Oxford/IRL Press. 113–151.
36. Walsh, A., Y. Ito, and J. L. Breslow. 1989. High levels of human apolipoprotein AI in transgenic mice result in increased plasma levels of small high density lipoprotein (HDL) particles comparable to human HDL3. *J. Biol. Chem.* 264:6488–6494.
37. Zechner, R. 1990. Rapid and simple purification of lipoprotein lipase from human breast milk. *Biochim. Biophys. Acta.* 1044:20–25.
38. Farquhar, M. G., and G. E. Palade. 1965. Cell junctions in amphibian skin. *J. Cell Biol.* 26:263–291.
39. Richardson, K. C., L. Jarett, and E. H. Finke. 1960. Embedding in epoxy resin for ultra-thin sectioning in electron microscopy. *Stain Technol.* 35:313–323.
40. Reynolds, E. S. 1963. The use of lead citrate at high pH as an electron opaque stain in electron microscopy. *J. Cell Biol.* 17:208–213.
41. Aalto-Setälä, K., C. L. Bisgaier, A. Ho, K. A. Kieft, M. G. Traber, H. J. Kayden, R. Ramakrishnan, A. Walsh, A. D. Essener, and J. L. Breslow. 1994. Intestinal expression of human apolipoprotein A-IV in transgenic mice fails to influence dietary lipid absorption or feeding behavior. *J. Clin. Invest.* 93:1776–1786.
42. Aalto-Setälä, K., E. Fisher, X. Chen, T. Chajek-Shaul, T. Hayek, R. Zechner, A. Walsh, R. Ramakrishnan, H. Ginsberg, and J. L. Breslow. 1992. Mechanism of hypertriglyceridemia in human apo CIII transgenic mice. *J. Clin. Invest.* 90:1889–1900.
43. Folch, J., M. Lees, and G. H. Sloane Stanley. 1957. A simple method for the isolation and purification of total lipids from animal tissues. *J. Biol. Chem.* 226:497–509.
44. Kates, M., B. Palameta, C. N. Joo, D. J. Kushner, and N. E. Gibbons. 1966. Aliphatic diether analogs of glyceride-derived lipids. IV. The occurrence of di-O-dihydrophytylglycerol ether containing lipids in extremely halophilic bacteria. *Biochemistry*. 5:4092–4099.
45. Weintraub, M. S., S. Eisenberg, and J. L. Breslow. 1987. Different patterns of postprandial lipoprotein metabolism in normal, type IIa, type III, and type IV hyperlipoproteinemic individuals. *J. Clin. Invest.* 79:1110–1119.
46. Levak-Frank, S., H. Radner, A. Walsh, R. Stollberger, G. Knipping, G. Hoefler, W. Sattler, N. Schachter, P. H. Weinstock, J. L. Breslow, and R. Zechner. 1995. Muscle specific overexpression of lipoprotein lipase causes a severe myopathy characterized by proliferation of mitochondria and peroxisomes in transgenic mice. *J. Clin. Invest.* 96:976–986.

47. Brun, L. D., C. Gagne, P. Julien, A. Tremblay, S. Moorjani, C. Bouchard, and P. J. Lupien. 1989. Familial lipoprotein lipase-deficiency: a study of total body fatness and subcutaneous fat tissue distribution. *Metab. Clin. Exp.* 38:1005-1009.
48. Lalouel, J., D. Wilson, and P. Iverius. 1992. Lipoprotein lipase and hepatic triglyceride lipase: molecular and genetic aspects. *Curr. Opin. Lipidol.* 3:86-95.
49. Smart, J. L., D. N. Stevens, J. Tonkiss, N. S. Auestad, and J. Edmond. 1984. Growth and development of rats artificially reared on different milk-substitutes. *Br. J. Nutr.* 52:227-237.
50. Peterson, J., G. Bengtsson-Olivecrona, and T. Olivecrona. 1986. Mouse preheparinized plasma contains high levels of hepatic lipase with low affinity for heparin. *Biochem. Biophys. Acta.* 878:65-70.
51. Komaromy, M. C., and M. C. Schotz. 1987. Cloning of rat hepatic lipase cDNA: evidence for a lipase gene family. *Biochemistry.* 84:1526-1530.
52. Cai, S. J., D. M. Wong, S. H. Chen, and L. Chan. 1989. Structure of human triglyceride lipase gene. *Biochemistry.* 28:8966-8971.
53. Yamamoto, N. 1993. Very low-density lipoprotein receptor (review). *Seikagaku J. Jpn. Biochem. Soc.* 65:557-561.
54. Jokinen, E. V., K. T. Landschulz, K. L. Wyne, Y. K. Ho, P. K. Frykman, and H. H. Hobbs. 1994. Regulation of the very low density lipoprotein receptor by thyroid hormone in rat skeletal muscle. *J. Biol. Chem.* 269:25411-25418.
55. Huttunen, L. V., C. Ehnholm, M. Kekki, and E. A. Nikkila. 1977. Post-heparin plasma lipoprotein lipase and hepatic lipase in normal subjects relationship to age, sex, and triglyceride metabolism. *Adv. Exp. Med. Biol.* 82:146-148.
56. Patsch, J. R., S. Prasad, A. M. Gotto, Jr., and W. Patsch. 1987. High density lipoprotein: relationship of the plasma levels of this lipoprotein species to its composition, to the magnitude of postprandial lipidemia, and to the activities of lipoprotein lipase and hepatic lipase. *J. Clin. Invest.* 80:341-347.
57. Goldberg, I. J., W. S. Blaner, T. Vanni, M. Moukides, and R. Ramakrishnan. 1990. The role of lipoprotein lipase in the regulation of high density lipoprotein catabolism. Studies in normal and lipoprotein lipase inhibited monkeys. *J. Clin. Invest.* 86:463-473.
58. Brinton, E. A., S. Eisenberg, and J. L. Breslow. 1994. Human HDL cholesterol levels are determined by apo A-I fractional catabolic rate which correlates inversely with estimates of HDL particle size. *Arterioscler. Thromb.* 14:707-720.
59. Hayek, T., N. Azrolan, R. Verdery, A. Walsh, T. Chajek-Shaul, L. Agellon, A. R. Tall, and J. L. Breslow. 1993. Hypertriglyceridemia and cholesterol ester transfer protein interact to dramatically alter high density lipoprotein levels, particle sizes, and metabolism. *J. Clin. Invest.* 92:1143-1152.
60. Laker, M. F. 1987. Plasma lipids and lipoproteins in diabetes mellitus. *Diabetes Annu.* 3:459-478.
61. Grundy, S. M., A. Chait, and J. D. Brunzell. 1987. Familial combined hyperlipidemia workshop. *Arteriosclerosis.* 7:203-207.
62. Williams, K., K. Petrie, R. Brocia, and T. Swenson. 1991. Lipoprotein lipase modulates net secretory output of apolipoprotein B in vitro. *J. Clin. Invest.* 88:1300-1306.